

Factors Affecting the Accuracy of SHOWEX HF Radar Wave Measurements

LUCY R. WYATT AND GUENNADI LIAKHOVETSKI

Sheffield Centre for Earth Observation Science, Department of Applied Mathematics, University of Sheffield, Sheffield, United Kingdom

HANS C. GRABER AND BRIAN K. HAUS

Rosenstiel School for Marine and Atmospheric Science, University of Miami, Miami, Florida

(Manuscript received 28 March 2003, in final form 30 August 2003)

ABSTRACT

Ocean Surface Current Radar (OSCR) HF radar measurements of ocean waves and currents were made during the Shoaling Waves Experiment (SHOWEX) in the fall of 1999. During some periods, at some locations, good quality wave measurements were obtained. Limitations in the wave measurement capability due to OSCR hardware, deployment configuration, signal-to-noise ratio, and antenna sidelobes are identified and discussed. A short period of large currents in the presence of antenna pattern distortion is identified as the source of the main errors in the wave measurements.

1. Introduction

Wave measurements are obtained from HF radar backscatter using the theoretical relationship between the ocean wave directional spectrum and the backscatter power spectrum developed by Barrick (1972), Barrick and Weber (1977), and Weber and Barrick (1977). Simple empirical relationships between the moments of the backscatter spectrum and equivalent moments of the ocean wave spectrum, for example, significant wave height and mean period, have been used (Barrick 1977; Wyatt 1988, 2002; Maresca and Georges 1980; Graber and Heron 1997; Heron and Heron 1998). These methods can be applied to data from a single radar system, although with some ambiguities in some of the parameters. Inverse methods have been developed to determine the directional spectrum (Lipa 1978; Wyatt 1990, 2000; Howell and Walsh 1993; Hisaki 1996; Hashimoto and Tokuda 1999). Although some of these methods have been applied to data from a single radar, robust measurements appear to need a dual-radar system (Wyatt 1987; Atanga and Wyatt 1997; Wyatt 2002). The Wyatt (1990, 2000) method has been subject to a num-

ber of experimental trials which have established the accuracy of the spectrum and derived parameters (Wyatt et al. 1999, 2003). Figure 1 shows a typical backscatter power spectrum (usually called a Doppler spec-

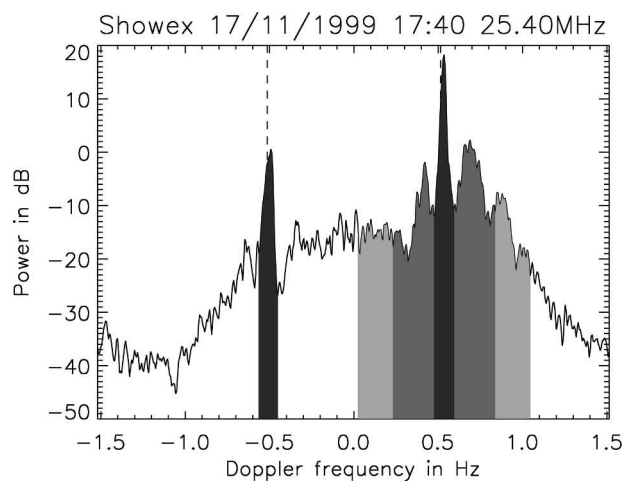


FIG. 1. Typical Doppler spectrum. First-order peaks, used for surface current and wind direction estimation, are shaded in black. The second-order spectrum, used for wave height and directional spectrum estimation, is in dark gray, and light gray indicates the additional second-order region used in mean period estimation. The noise level for this spectrum is about -40 dB. Signal-to-noise ratio is measured from the peak first- or second-order level.

Corresponding author address: Lucy R. Wyatt, Sheffield Centre for Earth Observation Science, University of Sheffield, Hicks Building, Hounsfield Road, Sheffield S3 7RH, United Kingdom. E-mail: l.wyatt@sheffield.ac.uk

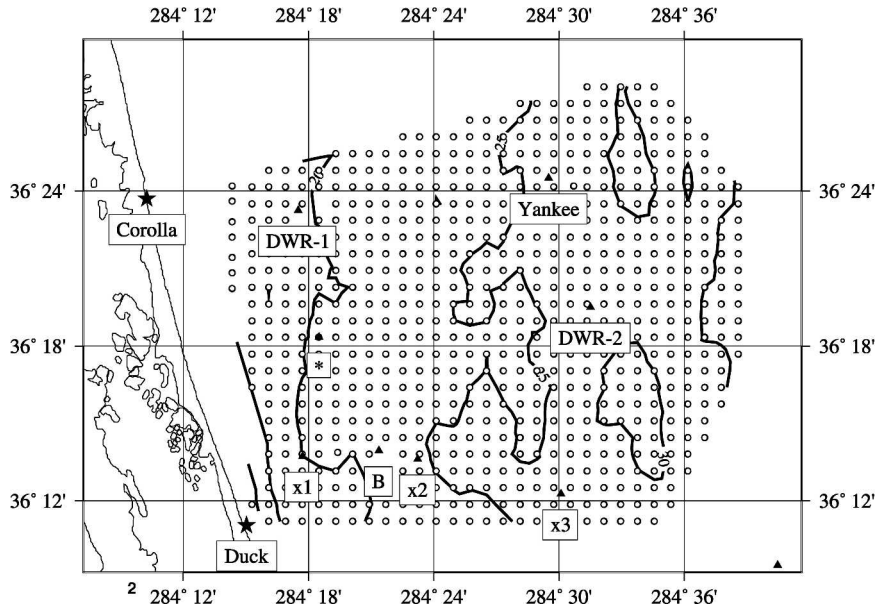


FIG. 2. Map showing SHOWEX measurement area, to mark OSCR measurement cells and device locations: X1, X2, X3, and dwr-1 are directional waveriders; dwr-2 is a Wavec directional buoy; B and Yankee are air-sea interaction spar (ASIS) buoys; asterisk (*) shows location of OSCR measurements used in some of the comparisons.

trum) and the way in which it is partitioned to provide wave, current, and wind measurements.

The Shoaling Waves Experiment (SHOWEX) provided another opportunity to do an evaluation, for the first time in the United States and on a coast exposed to

Atlantic Ocean swells. The aim of the experiment was to investigate the development of the directional wave spectrum as long ocean waves propagate into shallow coastal waters. A number of in situ wave measurement devices were deployed at various sites across the region

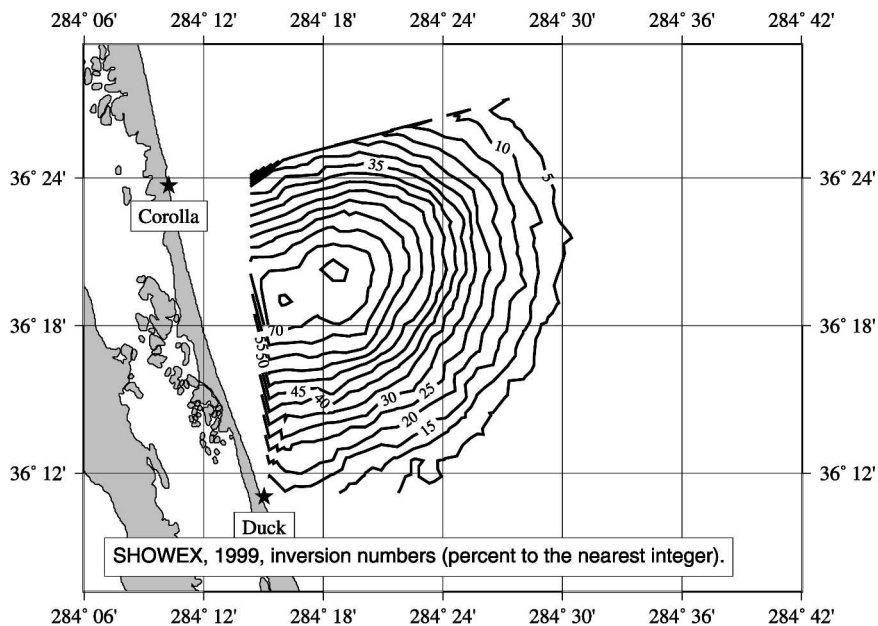


FIG. 3. OSCR wave data availability during SHOWEX. Contours show the percent of data that was suitable for inversion at each location.

(see Fig. 2). The University of Miami deployed their Ocean Surface Current Radar (OSCR) HF radar system at two sites in North Carolina, Corolla and Duck, with a view to obtaining surface current and wave information over a significant part of the experimental area. This paper discusses the wave measurements from this OSCR deployment, compares them with data from the directional waveriders, and identifies some of the factors that have limited both the availability of data and its accuracy.

The OSCR was developed by the U.K. Rutherford Appleton Laboratory in the early 1980s. A commercial version was developed first by Marex and then by Marconi, but there was very little further development during the 1990s. In particular, the computer system used (PDP-11s) has become very outdated and inflexible. This has not been a particular problem for surface current applications, but it is a limitation for the more demanding requirements of surface wave measurement. First attempts to make wave measurements with the system were carried out by Marconi in the late 1980s, and the data were subsequently also processed using the methods of Wyatt (1990) and Howell and Walsh (1993) (E. G. Pitt 1992, unpublished manuscript). This and further work with short OSCR datasets was reported in Wyatt and Ledgard (1996). The Doppler spectra stored in the OSCR system have limited dynamic range and poor Doppler sidelobes due to inadequate weighting in the Doppler processing and hence are not suitable for inversion. It was therefore necessary to download the raw data (or, rather, the in-phase and quadrature components of the radar signal after demodulation) and carry out the Doppler processing off-site. The OSCR software provides an option for data download, but the tape drive limitations mean that less than one day's data are obtained before local human operator intervention is needed.

None of this work involved collocated wave measurements, so only qualitative judgments on the accuracy were possible. During the winters of 1994/95 and 1995/96 OSCR systems were deployed on the U.K. Yorkshire coast at Holderness as part of an experiment to understand coastal erosion processes (Prandle et al. 1996). The aim here was to collect continuous data records over several weeks and make quantitative comparisons with directional wave buoys. This required an operator to be on-site every day in order to change the tapes. It became clear that the tape drives were not completely reliable, a number of tapes were corrupted, and continuous data collection was not achieved. Nonetheless the data that were collected showed good agreement with the collocated buoys most of the time (Wyatt et al. 1999).

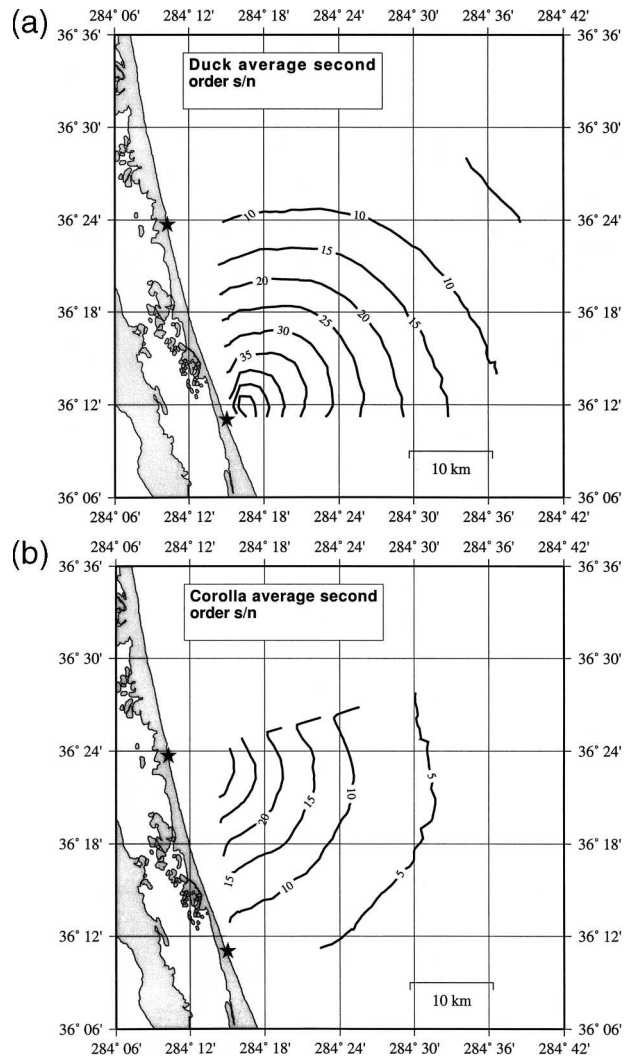


FIG. 4. Averaged second-order signal-to-noise ratio for the (a) Duck and (b) Corolla radars over the whole experiment.

The accuracy of the Holderness measurements, the problems with the OSCR hardware, and difficulties encountered in trying to upgrade the system were some of the motivations for the development of the German Wellen radar (WERA) radar (Gurgel et al. 1999). This radar has demonstrated round-the-clock operations for both currents and waves (Wyatt et al. 1999, 2003). More recently, the U.K. Pisces radar (Shearman and Moorhead 1988; M. D. Moorhead and L. R. Wyatt 2001, unpublished manuscript; M. D. Moorhead et al. 2002, unpublished manuscript) has also demonstrated a similar capability, although to much longer ranges (to 150 km offshore for waves). However, in SHOWEX it was an OSCR system that was deployed, and a system now some 5 yr older than the ones used at Holderness, and

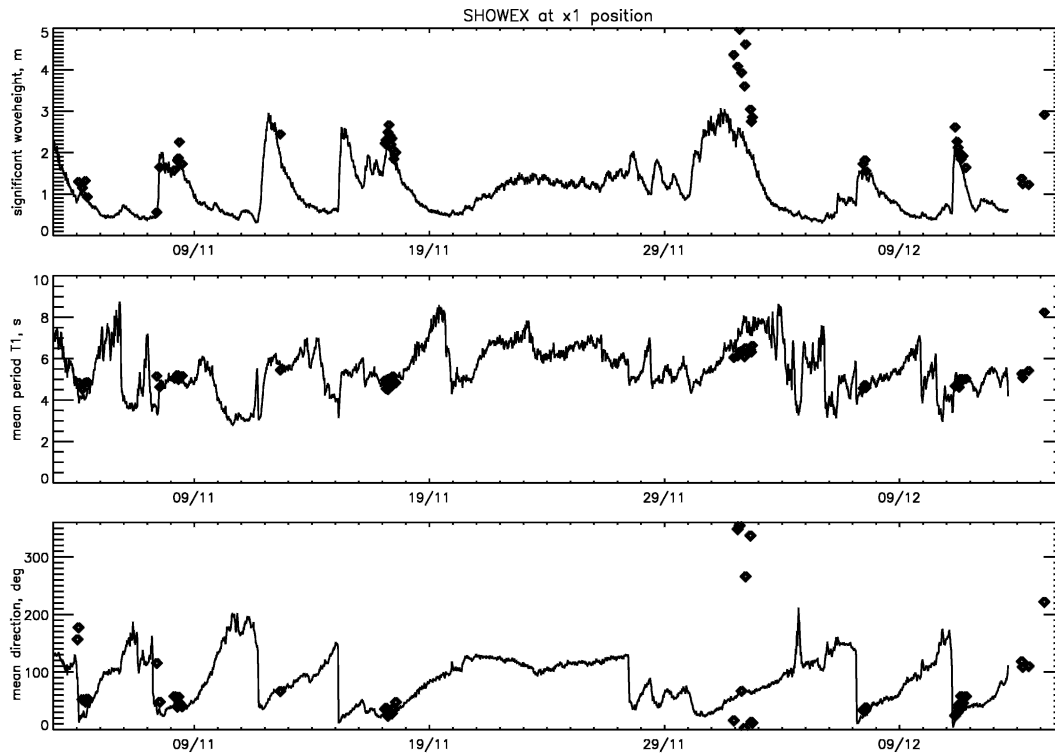


FIG. 5. Comparisons of significant wave height, mean period, and mean direction between OSCR (diamonds) and buoy (solid line) at the X1 position.

round-the-clock operation was not expected. In fact, the tape drives were so unreliable that there were unfortunately several long gaps in coverage.

Although SHOWEX was limited in the amount of HF radar data collected, it needs to be emphasized that this was due to the use of OSCR and not a property of HF radar in general. It was also different from other experiments in a particularly useful respect. In previous experiments the wave buoys have been deployed in the center of the region of HF radar coverage in order to maximize the radar data quality and availability in order to get reliable quantitative measures of HF radar wave measurement accuracy. In this experiment the buoys were deployed at the extremes of the radar coverage in order to meet the oceanographic science aims of the experiment. Thus, for the first time, it was possible to get some quantitative measures of the quality of HF radar wave measurements at the borders of the coverage region. Comparisons with Simulating Waves Nearshore (SWAN) wave model runs at Holderness (Caires 2000) suggested that accuracy was likely to be reduced due to signal-to-noise limitations and antenna sidelobe impacts. The aim of this paper is to discuss in more detail the evidence of these effects in the SHOWEX measurements.

2. Signal-to-noise ratio

Wave measurement requires a signal-to-noise ratio of at least 10 dB in the second-order part of the spectrum and, at the frequency of operation and the transmitted power of OSCR, this needed ideally a separation of about 15 km compared to the site separation of more like 25 km. Unfortunately, the decision to use the system for wave measurements was made rather late in the experimental planning and the sites that had been selected were rather far apart. To ensure that some wave measurements were possible the pulse length was doubled, from $6.667 \mu\text{s}$, to give an expected signal-to-noise gain of 6 dB, with the result that neighboring measurement cells, with spatial separations of 1 km, were more correlated than is usual in an OSCR deployment. This section discusses the consequences on data availability. Figure 3 shows the amount of data returned at each location over the area. Contours are drawn at increments of 5%. This shows that changing the pulse length did provide for 70% or more data return in the center of the coverage but that this dropped to 20% or less in the vicinity of the wave buoys.

The main factor in determining wave data availability is a second-order signal-to-noise ratio, which depends

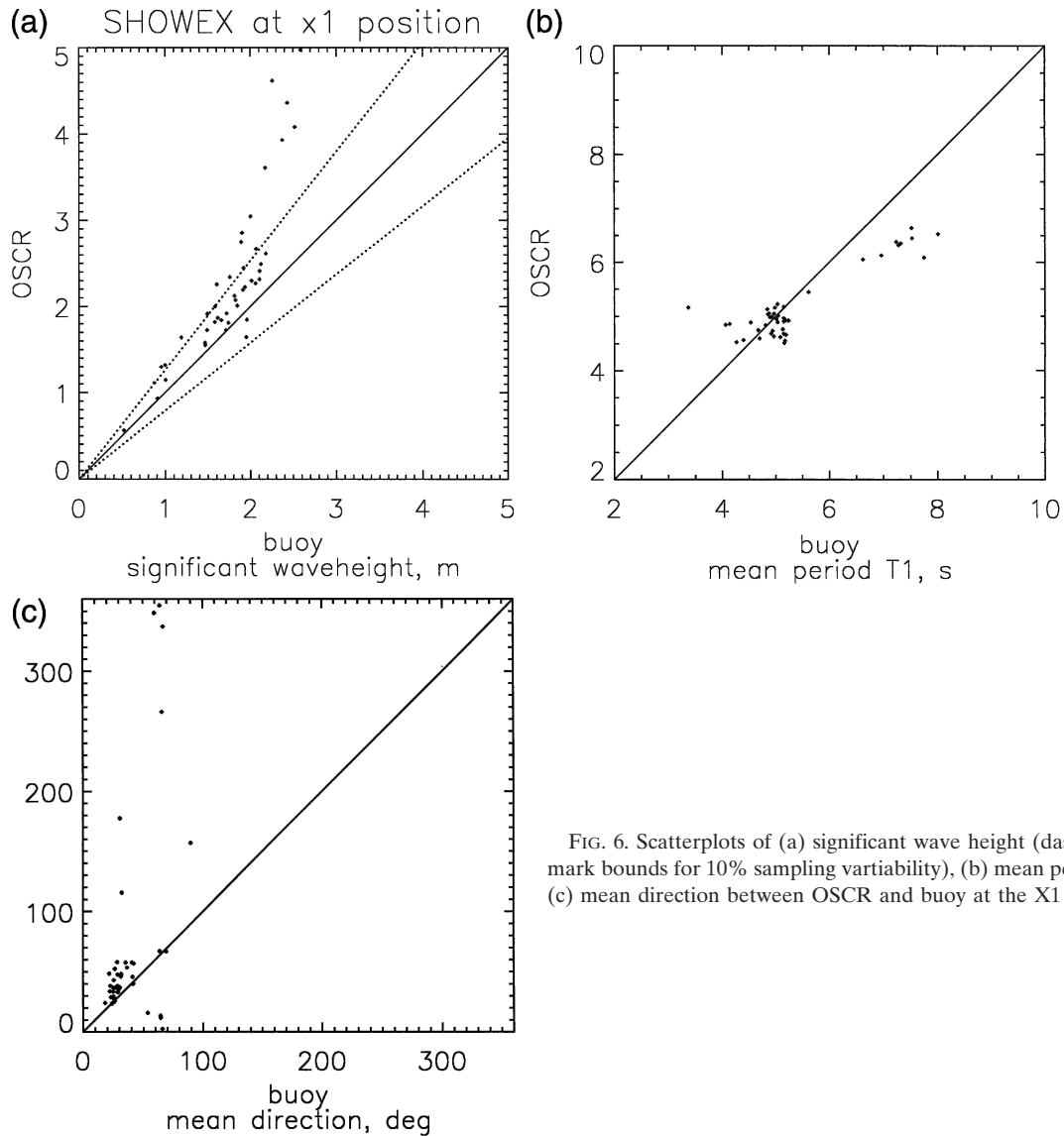


FIG. 6. Scatterplots of (a) significant wave height (dashed lines mark bounds for 10% sampling variability), (b) mean period, and (c) mean direction between OSCAR and buoy at the X1 position.

on factors such as background noise, the external interference environment, wind direction, and wave height. A more detailed exploration of the impact of these factors has been undertaken recently using the Pisces radar (M. D. Moorhead et al. 2002, unpublished manuscript), but these results are not all transferable to the OSCAR case because of the difference in frequency of operation. Figure 4 shows second-order signal-to-noise measurements for the two sites averaged over the whole experiment. The signal-to-noise ratio reduces with range as the signal returned to the radar is subject to attenuation over the longer sea path from long ranges. The maximum signal-to-noise ratio at the Duck radar is about 50 dB, which is about the same as OSCAR at Holderness. However, the maximum at the Corolla

site is rather less, at 35 dB, due to power supply problems (the source of which was not identified) at this site; that is, it is the signal level that is lower rather than the noise being higher. Whereas from Duck the 10-dB requirement is achieved (on average) to about 25 km, the area covered by 10 dB or more from Corolla is much smaller and hence the region of overlap, that is, where both radars have signal-to-noise ratios greater than 10 dB so that directional spectrum measurement is possible, is rather small and is consistent with the data return percentages shown in Fig. 3. In previous experiments we have in fact set a higher signal-to-noise limit of 15 dB. Figure 4 shows that if we had kept this quality requirement we would have had even fewer directional spectra measurements.

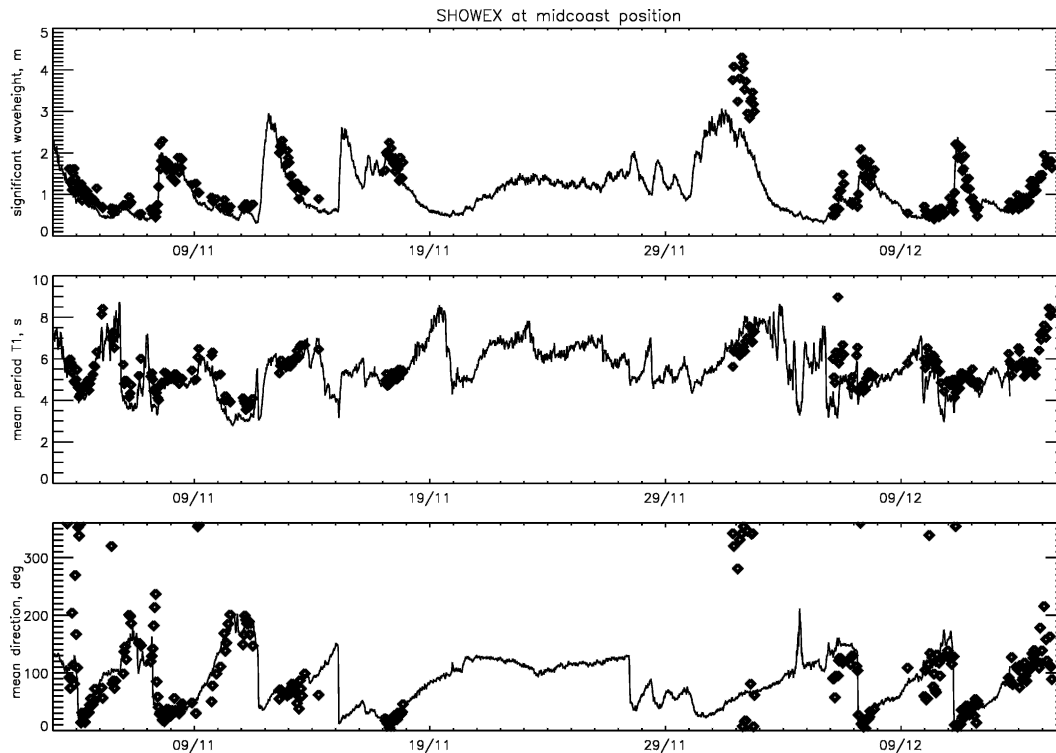


FIG. 7. Comparisons of significant wave height, mean period, and mean direction between OSCR (diamonds) at the point * between the two radars and the buoy (solid line) at the X1 position.

3. The OSCR wave measurements

The signal-to-noise plots show that the directional waveriders at X1 and X2 were well within the expected range of the OSCR located at Duck but at the extreme edge of expected coverage from the northern site at Corolla. Only 26 directional spectra measurements were possible with OSCR at X2, a slightly longer range from Corolla, compared to 44 at X1. Figure 5 shows a comparison of some wave parameters at X1. Scatterplots of these are presented in Fig. 6. It is clear that the OSCR wave parameter estimates at this location are not very accurate. Wave heights are too high (a relative bias of 27%), although they are correlated with those of the buoy, with a correlation coefficient of 0.85. Periods have a correlation coefficient of 0.9, but the range of values is not large enough to quantify the relationship with the buoy with any confidence. The mean directions are rather scattered, although most of the radar measurements are fairly close to those of the buoy (mean difference of 19°). These sorts of differences are similar to those seen in the model comparisons (Caires 2000) and are probably due to the Corolla radar signal-to-noise limitations.

The most striking feature of the comparison is the data on 2 December 1999, when the overestimation in

wave height is much larger and the other parameters are also in worse agreement. Overestimations in wave height of this magnitude have been found in previous work (Wyatt et al. 1999, 2003), although not when wave heights are as low as 3 m, so this SHOWEX result is a much larger error than previously encountered. One possible explanation is that the lower signal-to-noise threshold of 10 dB used in these measurements is too low (a more compelling explanation is discussed in section 4). However, comparisons between the X1 buoy wave parameters and OSCR parameters measured at a location farther to the north (identified with an asterisk in Fig. 2), where signal-to-noise levels could be expected to be mostly above the 15-dB criterion (see Figs. 7 and 8), show a similar anomalous behavior on 2 December. Furthermore, signal-to-noise levels on this particular day appeared to be higher than normal. Notice that at this location there are 231 directional spectra for comparison. The relative bias in wave height is 19%, with a correlation coefficient of 0.9. Periods have a correlation coefficient of 0.75, with a tendency for underestimating high periods and overestimating low. The mean directions are rather scattered, although the radar measurements are better correlated with the buoy at this location and have a mean difference of less than 1° .

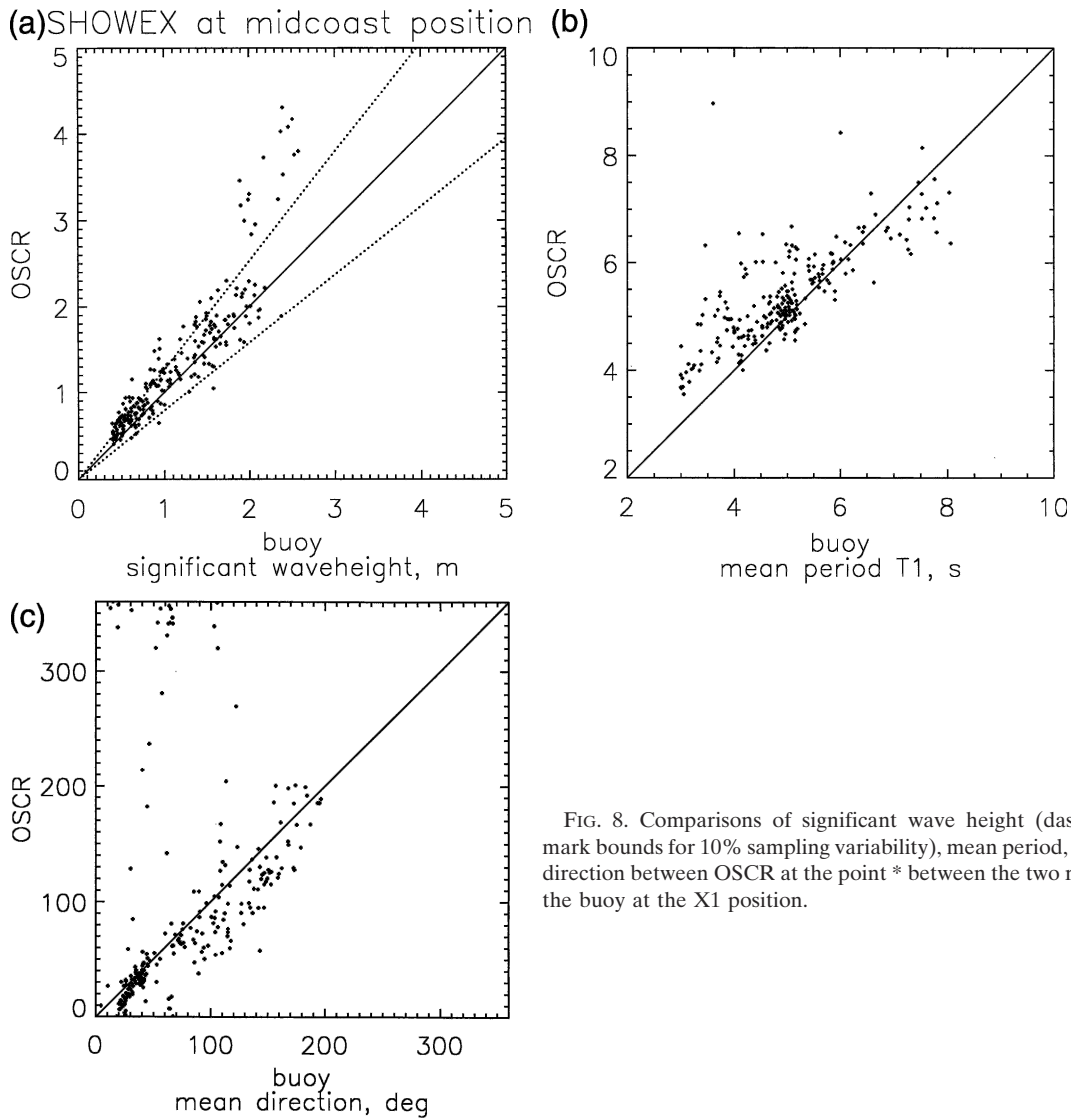


FIG. 8. Comparisons of significant wave height (dashed lines mark bounds for 10% sampling variability), mean period, and mean direction between OSCR at the point * between the two radars and the buoy at the X1 position.

Figure 9 shows directional spectra at hourly intervals during a day (17 November) when wave parameter comparisons between radar [at asterisk (*)] and buoy (at X1) are quite good. The buoy spectra were generated using the Lygre and Krogstad (1986) maximum entropy method, which tends to give rather peaky distributions; hence, peak amplitudes in the buoy spectra are often larger than those measured by the radar. Note that, apart from this peakiness, Krogstad et al. (1999) show that the overall shape of directional spectra obtained with this method is good. There are few changes in either buoy or radar spectra during the day, and agreement in both shape and amplitude is rather good. However, comparisons of directional spectra on 2 December are poor (Fig. 10), thus explaining the poor agreement in wave parameters. Differences in direc-

tional spectra of this magnitude have been seen before but most commonly in high sea states with wave heights of 6 m or more. These have been attributed to limitations of Barrick's equations in highly nonlinear seas, and methods to deal with this are under investigation. On this occasion wave heights were less than 3 m, so this is not an explanation. Antenna sidelobes (also identified in earlier work) are a more likely explanation in this case. These are discussed further in the following section.

4. Antenna sidelobes

Previous experiments with OSCR have made clear that careful measurement and calibration of the receive array is needed in order to minimize antenna sidelobe

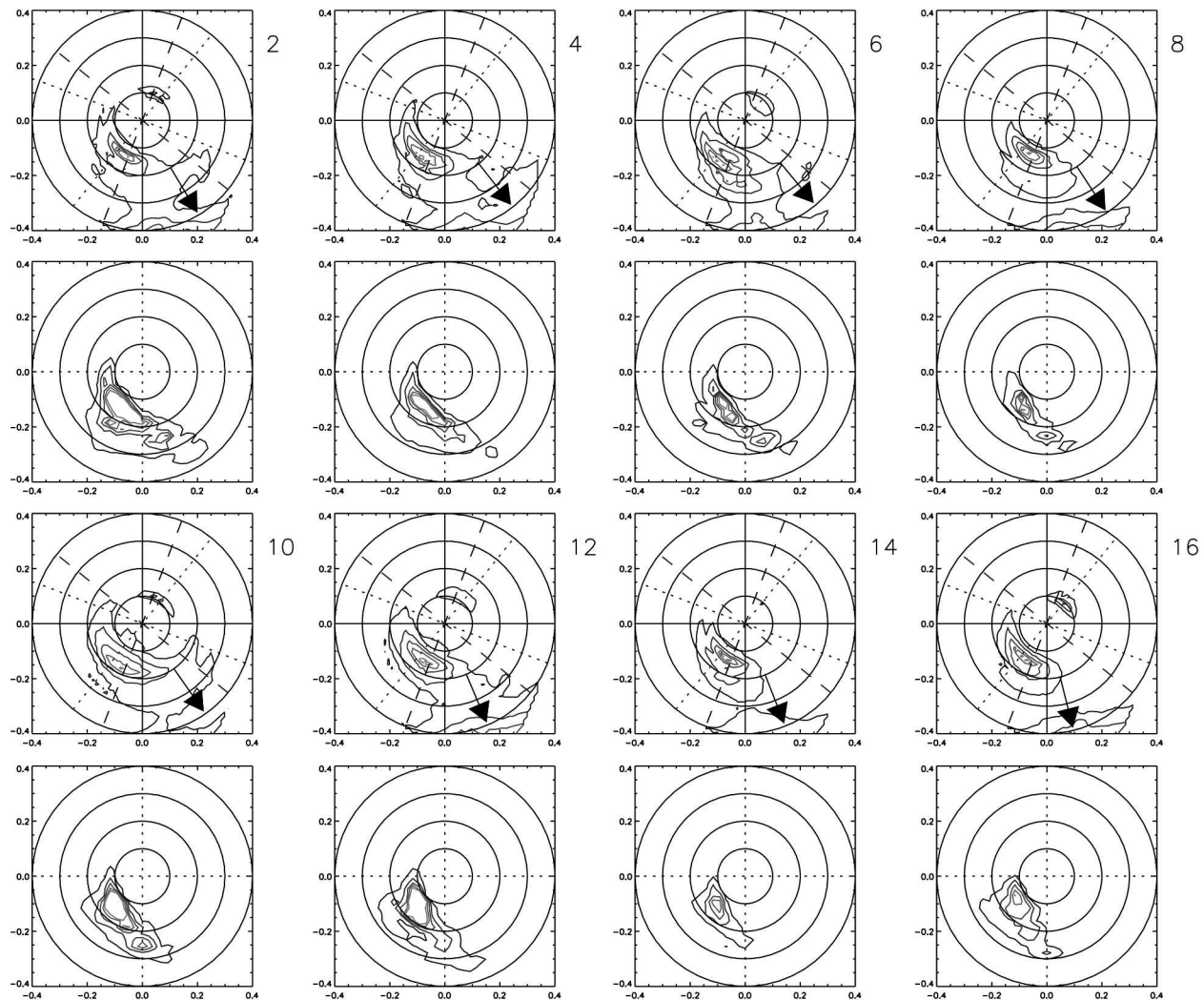


FIG. 9. Directional spectra measured by (top) OSCR and (bottom) the directional waverider at the X1 position on 17 Nov 1999, with time (in h) (shown to the right of the OSCR spectrum) increasing from left to right and from top to bottom. Each pair is scaled in magnitude relative to the maximum value in the radar spectrum. The arrow shows the OSCR wind direction measurement.

levels. Kingsley et al. (1997) showed that the angle between the array and the coastline can be important, and, if they are not aligned, both phase and amplitude compensation may be needed. Experiments at Holderness, showed that careful on-site measurements combined with radiation-pattern modeling gives results similar to antenna fields measured using a transponder on a ship steered around the array. During SHOWEX the antenna array patterns were not measured. The antenna array at the Corolla site was fairly well aligned with the coastline, but there were occasional problems with animal damage to the cables. The array at Duck was at more of an angle and the elements were difficult to get to through gorse bushes. Although considerable effort was made to improve the cabling at both sites at the beginning of the experiment, the results presented

in this section suggest that the antenna patterns at both sites were often rather poor, with sidelobes much higher than the 23 dB that might be expected from the cosine weighting used in OSCR beam forming.

Sidelobe problems are most obvious when there is a large surface current, which leads to different radial currents and hence different first-order Doppler shifts in different look directions. Surface radial currents obtained using a simple peak search algorithm from the Doppler spectra from both sites suggest a large current from the northeast on 2 December. This is probably associated with a coastal buoyancy current, a feature that has been seen before in this area under similar wind conditions. A decrease in salinity was reported by the U.S. Army Corps of Engineers Field Research Facility (FRF) at Duck.

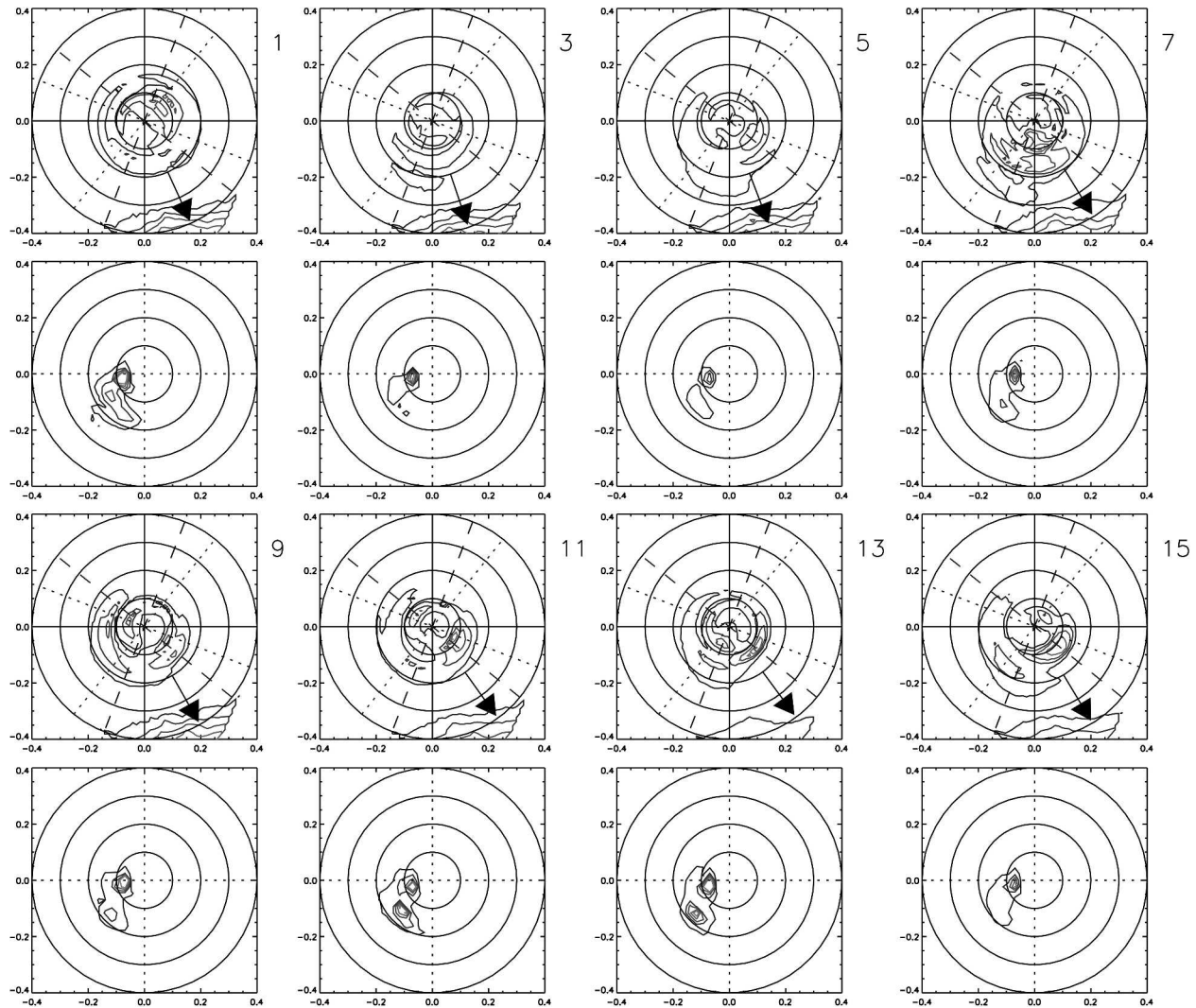


FIG. 10. Directional spectra measured by (top) OSCR and (bottom) the directional waverider at the X1 position on 2 Dec 1999, with time (in h) (shown to the right of the OSCR spectrum) increasing from left to right and from top to bottom. Each pair is scaled by magnitude relative to the maximum value in the radar spectrum. The arrow shows the OSCR wind direction measurement.

When there are large differences in first-order Doppler shifts, the Bragg peak in one direction (A, say) at one range can then appear in the spectrum in another direction (B, say) at the same range, separated from the B Bragg peak. If the beam forming were perfect, the A peak would be suppressed in the B spectrum and, except in very low seas, would not be much of a problem. When the suppression is lessened, the A Bragg peak appears as a significant part of the wave signal in the B spectrum. An example is shown in Fig. 11 that should be compared with Fig. 1, in which there is little evidence of antenna sidelobe problems. These data are for 2 December 1999, when radar significant wave heights and directional distributions are very different from those of the directional waveriders. Doppler spectra

were examined at all locations at a distance of about 12 km from the two radar sites respectively (the selected locations are shown in Fig. 12). The Bravo and X2 buoys were located at about this distance from the Duck site and the dwr1 buoy at about 12 km from the Corolla site. The figure shows only spectra from the Duck site at the location closest to the coast (cell 4), near the Bravo location (cell 152), and near the X1 location (cell 193), but this is sufficient to get an idea of the impact of the antenna sidelobes. At cell 4 (Fig. 11a) the signals coming in on the sidelobes (dashed lines in the figure) are almost as large as the first-order Bragg peaks. At cell 152 (Fig. 11b) the second-order peaks around the main Bragg peak may be associated with sidelobes, although the effect is smaller. The lower

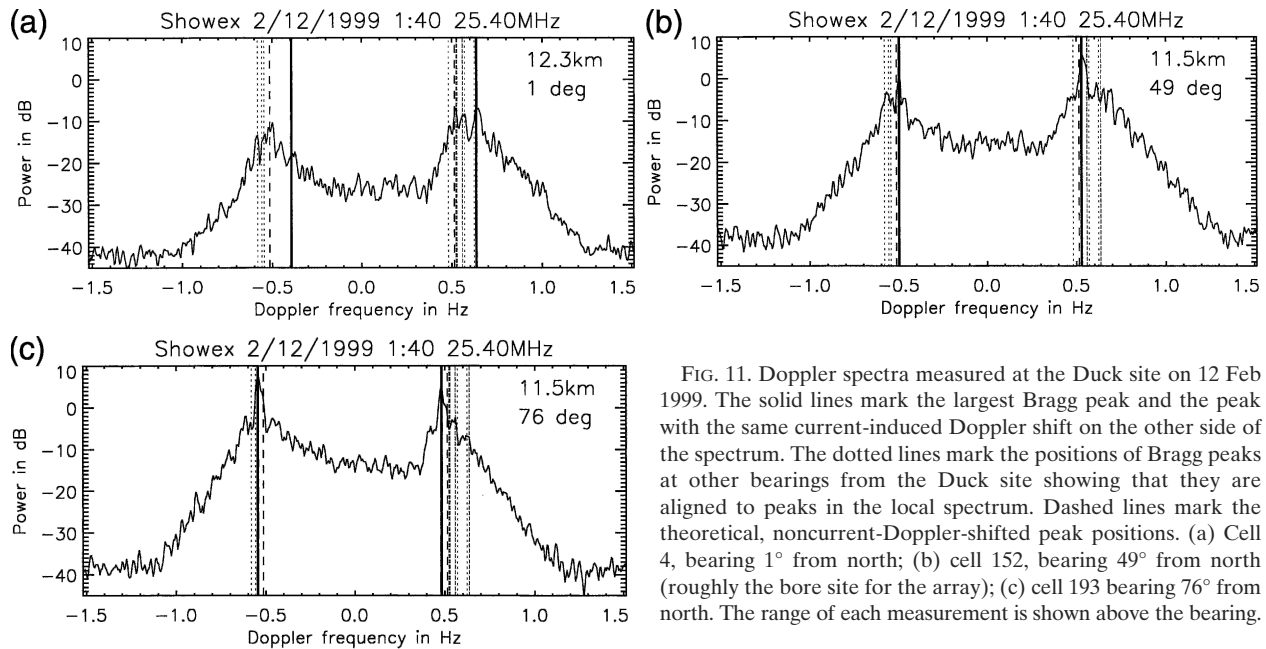


FIG. 11. Doppler spectra measured at the Duck site on 12 Feb 1999. The solid lines mark the largest Bragg peak and the peak with the same current-induced Doppler shift on the other side of the spectrum. The dotted lines mark the positions of Bragg peaks at other bearings from the Duck site showing that they are aligned to peaks in the local spectrum. Dashed lines mark the theoretical, noncurrent-Doppler-shifted peak positions. (a) Cell 4, bearing 1° from north; (b) cell 152, bearing 49° from north (roughly the bore site for the array); (c) cell 193 bearing 76° from north. The range of each measurement is shown above the bearing.

Bragg peak is also affected. In the direction at cell 193 (Fig. 11c) the wind is blowing away from the radar (larger peak at negative Doppler frequency), and the effect of the sidelobes is much less serious since it is only clearly evident around the lower Bragg peak (at positive Doppler frequency), which is not used for wave measurement.

The clear evidence of peaks in the local spectrum

associated with Bragg peaks from a different direction can be used to get a rough estimate of the antenna patterns associated with particular look directions. This is obtained in the following way. A look direction and range are selected, and the frequency of the peak in its Doppler spectrum is identified. The amplitude at this frequency in Doppler spectra for all other directions at approximately the same range is obtained. These am-

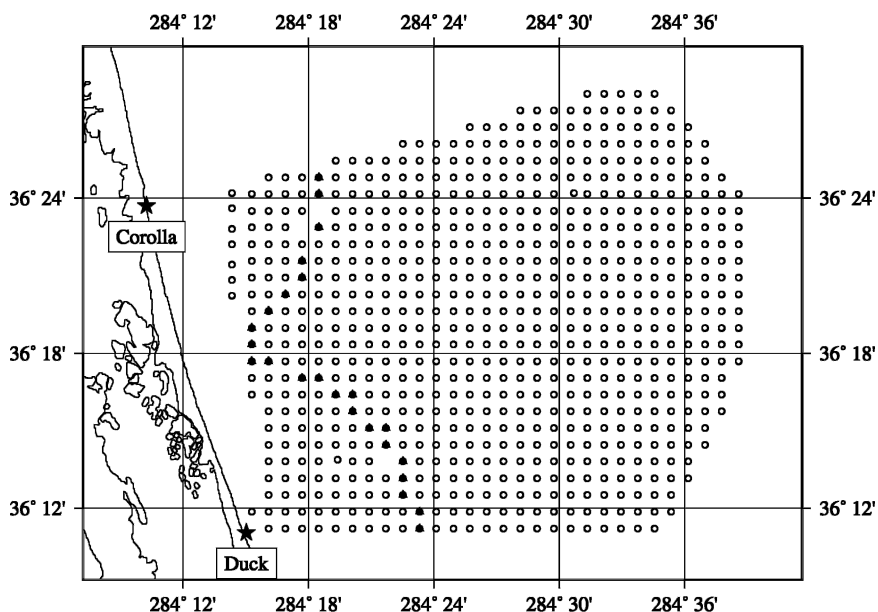


FIG. 12. Locations of Doppler spectra measurements (solid circles) used in the estimation of the antenna beam patterns from each site.

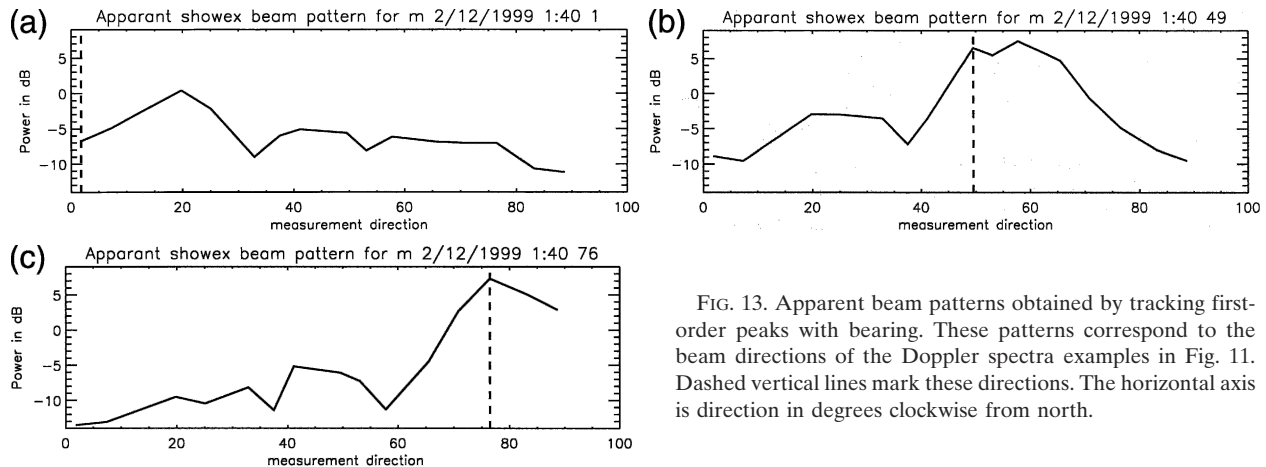


FIG. 13. Apparent beam patterns obtained by tracking first-order peaks with bearing. These patterns correspond to the beam directions of the Doppler spectra examples in Fig. 11. Dashed vertical lines mark these directions. The horizontal axis is direction in degrees clockwise from north.

plitudes are assumed to be associated with sidelobes of the antenna pattern in the chosen look direction. Figure 12 shows the locations used for the analysis. This will give a worst-case picture because in some directions the spectral amplitudes at the Bragg peak frequency for another direction will have significant local second-order contributions or, indeed, a smaller first-order peak. There will also be uncertainties because the ranges are not exactly equal in each direction. Examples are shown in Fig. 13. The pattern for the 1° beam shown in the upper panel is very similar to one obtained at 19° (not shown) because the position of the Bragg peak does not change much between these directions and the amplitudes are larger at 19°. What the figure shows is that at 19° (about 30° from bore site) the first sidelobe could be less than 10 dB down on the

main lobe. In the other two directions there are still significant sidelobes with minimum levels achieved not on bore site, as might have been expected, but on the 76° beam.

The interpretation presented above of the contributions to the Doppler spectra are substantiated in Fig. 14, which shows the Doppler spectra again (now normalized to the theoretical Bragg frequency and current removed) compared with spectra obtained by integrating Barrick's second-order equations using data from the X2 buoy. At cell 4 there is significant disagreement, so it is clear that the second-order signal is predominantly associated with antenna sidelobes, whereas at cell 152 the measurement and simulation are closer and the main contributions around the main Bragg peak are primarily the local waves. The sidelobe impact on the

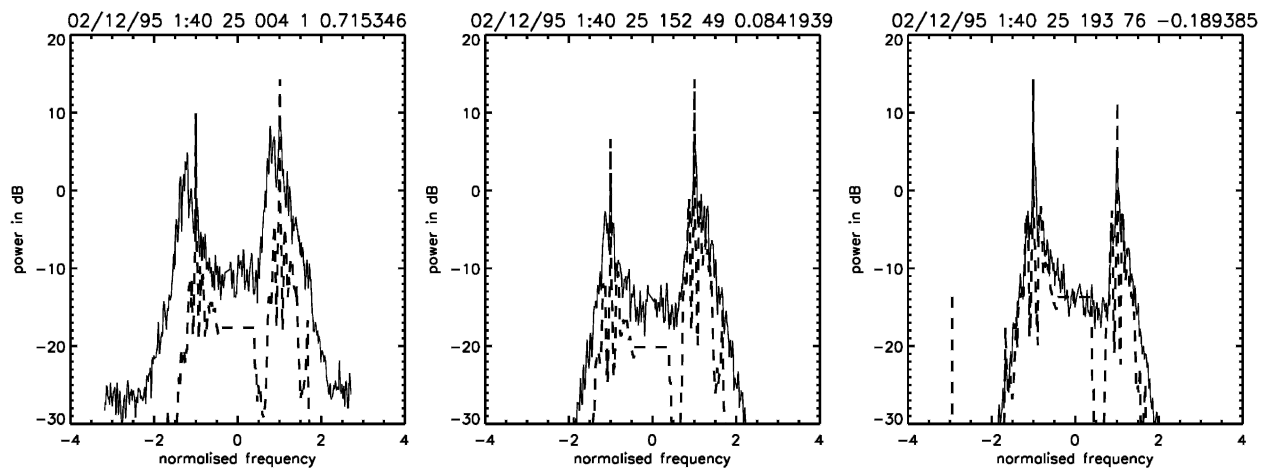


FIG. 14. Doppler spectra as in Fig. 11 with the frequency normalized by the Bragg frequency. The dashed lines show Doppler spectra simulated using buoy data and Barrick's second-order theory: (a) cell 4, bearing 1° from north; (b) cell 152, bearing 49° from north (roughly the bore site for the array); and (c) cell 193 bearing 76° from north. The number to the right above each figure is the radial current (in $m s^{-1}$) measured at that location.

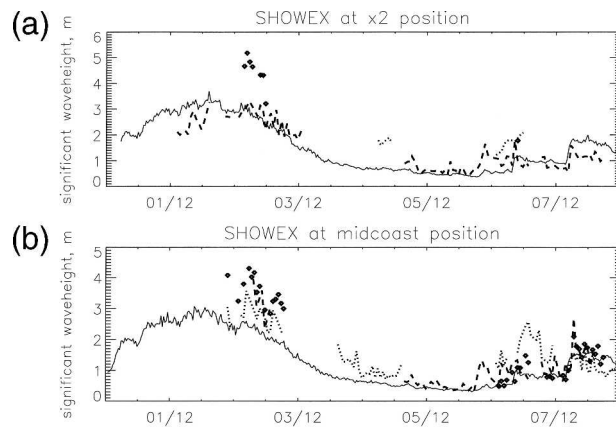


FIG. 15. Significant wave height, for the beginning of Dec 1999, estimated from the Duck Doppler spectra at the X2 buoy and at the location marked with an asterisk (*) in Fig. 2. Solid line is the buoy data (at X2 and X1, respectively); dashed line is the single-radar measurements from Duck; dotted line is the single radar from Corolla; and the diamonds are the dual-radar measurements.

lower Bragg peak at cell 152 is, however, clear. As expected, there is fairly good agreement between radar and model at cell 193.

Large sidelobes of the type identified here are interpreted as wave signals in the inversion, leading to overestimation of wave height and often spurious contributions to the wave directional spectrum, leading to errors in mean directions. The results presented above suggest that the Doppler spectra from the Duck radar site were not seriously influenced by sidelobe effects at the locations of Bravo and X2. However, the Corolla data at these locations suffer from a combination of poor signal-to-noise ratio and antenna sidelobe contamination. The bearing from the Corolla radar to these locations has similar sidelobe characteristics to the case shown in Fig. 11a. It was noted earlier that significant wave height was overestimated over the whole region on 12 February 1999. A particular point in the middle of the region (asterisk in Fig. 2) was selected for some of the comparisons shown earlier. Here the signal-to-noise ratio for both radars is similar, and the best wave measurements were expected. But this point was too close to the coast, and sidelobe effects similar to those in Fig. 11a dominate the result for both radars.

This is one occasion when wave height estimation from one radar only could give a more accurate result in the directions not affected by sidelobes. Single radar wave heights (using existing algorithms) are most accurate when the waves are propagating toward the radar. On 2 December wind directions were roughly toward the Duck radar at the X2 buoy, and the wave height comparison in Fig. 15 confirms that the wave height measured by the Duck radar was more accurate than

the dual-radar value, which, at this location, is affected by both poor signal-to-noise ratio and sidelobe problems from the Corolla radar. The corresponding figure for the middle of the region (asterisk in Fig. 2), where both radars are affected by sidelobes, shows that both single- and dual-radar wave height estimates are poor on 2 December. Note that in these figures there appear to be dual-radar measurements at times when only one signal radar measurement has been made. One reason for this is that the mean noise level is measured in a different way in the single- and dual-radar algorithms. This has an influence when signal-to-noise ratio is marginal. Second, the dual-radar processing has an algorithm for detecting and remedying some first-order Bragg peak problems that cause the single-radar processor to reject the data.

5. Discussion

This work, together with earlier work at Holderness in the United Kingdom (Wyatt et al. 1999), demonstrates that, although some wave measurement is possible, the OSCR HF radar is not capable of operational wave measurement. This is in contrast to other systems, for example, WERA and Pisces, that have demonstrated an operational capability (Wyatt et al. 1999; M. D. Moorhead et al. 2002, unpublished manuscript). The poor availability of HF radar wave data during SHOWEX is specific to the system used and should not be seen as a problem inherent to HF radar systems.

The measurements do identify two factors that are more generally important in evaluating HF radar wave measurements. The first of these is signal-to-noise ratio. There is a tendency for the methods used to overestimate significant wave height and to produce noisy direction estimates when the signal-to-noise ratio is poor, although, for this experiment, it is difficult to isolate this factor from the second, which arises due to poor antenna sidelobe control. The measurements suggest that sidelobe levels were very high during the experiment and led to the significant overestimation in wave height on 2 December 1999 associated with a very strong current from the northeast. Consistent overestimates of this magnitude have not been seen in previous work with OSCR, although some sidelobe problems were found (Kingsley et al. 1997). The results emphasize the importance of measuring the antenna pattern before an experiment and compensating where possible for any limitations in the pattern. Problems with the antenna pattern were likely to have been present throughout the experiment and will have degraded the accuracy of the wave parameters at times other than 2 December. However, as is clear with the measurements

on 17 November, reasonable results can still be obtained when the surface current is weaker.

Acknowledgments. The HF radar deployment and data collection were organized and staffed by Hans Graber's group at the University of Miami. We are grateful to Jim Green and Lesley Binks in SCEOS for their assistance in processing and archiving the HF radar data at Sheffield. Simon Kingsley, then in the Department of Electronic and Electrical Engineering at Sheffield, provided technical assistance during the installation period and suggested the change in pulse length to maximize range. We are grateful to Tom Herbers, Naval Postgraduate School, for the directional wave-aver data and to the U.S. Office of Naval Research for funding the work under Contract N000149911092.

REFERENCES

- Atanga, J., and L. R. Wyatt, 1997: Comparison of inversion algorithms for HF radar wave measurements. *IEEE J. Oceanic Eng.*, **22**, 593–603.
- Barrick, D. E., 1972: First-order theory and analysis of MF/HF/VHF scatter from the sea. *IEEE Trans. Antennas Propag.*, **AP-20**, 2–10.
- , 1977: Extraction of wave parameters from measured HF radar sea-echo Doppler spectra. *Radio Sci.*, **12**, 415–424.
- , and B. L. Weber, 1977: On the nonlinear theory for gravity waves on the ocean's surface. Part II: Interpretation and applications. *J. Phys. Oceanogr.*, **7**, 11–21.
- Caires, S., 2000: Comparative study of HF radar measurements and wave model hindcasts in shallow waters. Ph.D. thesis, University of Sheffield, 249 pp.
- Graber, H. C., and M. L. Heron, 1997: Wave height measurement from HF radar. *Oceanography*, **10**, 90–92.
- Gurgel, K.-W., G. Antonischki, H.-H. Essen, and T. Schlick, 1999: Wellen Radar (WERA): A new ground-wave HF radar for ocean remote sensing. *Coastal Eng.*, **37**, 219–234.
- Hashimoto, N., and M. Tokuda, 1999: A Bayesian approach for estimating directional spectra with HF radar. *Coastal Eng. J.*, **41**, 137–149.
- Heron, S. F., and M. L. Heron, 1998: A comparison of algorithms for extracting significant wave height from HF radar ocean backscatter spectra. *J. Atmos. Oceanic Technol.*, **15**, 1157–1163.
- Hisaki, Y., 1996: Nonlinear inversion of the integral equation to estimate ocean wave spectra from HF radar. *Radio Sci.*, **31**, 25–39.
- Howell, R., and J. Walsh, 1993: Measurement of ocean wave spectra using narrow beam HF radar. *IEEE J. Oceanic Eng.*, **18**, 296–305.
- Kingsley, S. P., T. M. Blake, A. J. Fisher, L. J. Ledgard, and L. R. Wyatt, 1997: Dual HF radar measurements of sea waves from straight coastlines. *Proc. Seventh Int. Conf. on HF Radio Systems and Techniques*, Nottingham, United Kingdom, IEE, 330–333.
- Krogstad, H. E., J. Wolf, S. P. Thompson, and L. R. Wyatt, 1999: Methods for the intercomparison of wave measurements. *Coastal Eng.*, **37**, 235–258.
- Lipa, B. J., 1978: Inversion of second-order radar echoes from the sea. *J. Geophys. Res.*, **83**, 959–962.
- Lygre, A., and H. E. Krogstad, 1986: Maximum entropy estimation of the directional distribution in ocean wave spectra. *J. Phys. Oceanogr.*, **16**, 2052–2060.
- Maresca, J. W., Jr., and T. M. Georges, 1980: Measuring rms wave height and the scalar ocean wave spectrum with HF skywave radar. *J. Geophys. Res.*, **85**, 2759–2771.
- Prandle, D., and Coauthors, 1996: The Holderness Coastal Experiment '93–'96. Proudman Oceanographic Laboratory Rep. 44, 48 pp.
- Shearman, E. D. R., and M. D. Moorhead, 1988: Pisces: A coastal ground-wave radar for current, wind and wave mapping to 200km ranges. *Proc. IGARSS'88*, Edinburgh, United Kingdom, IEEE, 773–776.
- Weber, B. L., and D. E. Barrick, 1977: On the nonlinear theory for gravity waves on the ocean's surface. Part I: Derivations. *J. Phys. Oceanogr.*, **7**, 3–10.
- Wyatt, L. R., 1987: Ocean wave parameter measurements using a dual-radar system: A simulation study. *Int. J. Remote Sens.*, **8**, 881–891.
- , 1988: Significant waveheight measurement with HF radar. *Int. J. Remote Sens.*, **9**, 1087–1095.
- , 1990: A relaxation method for integral inversion applied to HF radar measurement of the ocean wave directional spectrum. *Int. J. Remote Sens.*, **11**, 1481–1494.
- , 2000: Limits to the inversion of HF radar backscatter for ocean wave measurement. *J. Atmos. Oceanic Technol.*, **17**, 1651–1666.
- , 2002: An evaluation of wave parameters measured using a single HF radar system. *Can. J. Remote Sens.*, **28**, 205–218.
- , and L. J. Ledgard, 1996: OSCAR wave measurement—Some preliminary results. *IEEE J. Oceanic Eng.*, **21**, 64–76.
- , S. P. Thompson, and R. R. Burton, 1999: Evaluation of HF radar wave measurement. *Coastal Eng.*, **37**, 259–282.
- , and Coauthors, 2003: Validation and intercomparisons of wave measurements and models during the EuroROSE experiments. *Coastal Eng.*, **48**, 1–28.